

**Towards Understanding the Origin of Cosmic-Ray Positrons**  
**- SUPPLEMENTAL MATERIAL -**

(AMS Collaboration)

For references see the main text.

To distinguish positrons from charge confusion electrons, a charge confusion estimator  $\Lambda_{\text{CC}}^e$  is defined using the technique similar to that of Ref. [22]. The estimator combines several measurements: the ratio of the energy from the calorimeter to the momentum from the tracker,  $E/p$ , the track  $\chi^2/\text{d.o.f.}$ , momenta reconstructed with different combinations of tracker layers, the number of hits in the vicinity of the track, and the charge measurements in the TOF and in the tracker. With this method, positrons, which have  $\Lambda_{\text{CC}}^e \simeq +1$ , are efficiently separated from charge confusion electrons, which have  $\Lambda_{\text{CC}}^e \simeq -1$ . It also provides additional proton rejection by effectively using the ratio  $E/p$ :  $\Lambda_{\text{CC}}^e \simeq -1$ , if  $E/p$  is close to 0.

The comparison between the data and the Monte Carlo simulation for the fraction of charge confusion electrons (i.e. those reconstructed with the positive charge sign due to the finite tracker resolution or interactions in the detector materials) is presented in Fig. S1 for  $\Lambda_{\text{CC}}^e > 0$ .

The charge confusion in data is obtained using the template fitting technique described in the Letter. From the fit to the positive rigidity sample, we obtain the number of positron signal events  $N_{e^+}$ , charge confusion electron background events  $N_{e^-}^{\text{c.c.}}$ , and proton background events. From the fit to the negative rigidity sample, we obtain the number of electron signal events  $N_{e^-}$ , charge confusion positron background events  $N_{e^+}^{\text{c.c.}}$ , and proton background events. The charge confusion fraction in the data is calculated as  $N_{e^-}^{\text{c.c.}}/(N_{e^-}^{\text{c.c.}} + N_{e^-})$ .

The charge confusion in Monte Carlo simulation is directly calculated as the fraction of electrons being reconstructed with positive rigidity after the same selection cuts as used in data are applied.

TABLE SI: The positron flux  $\Phi_{e^+}$  as a function of the energy  $E$  at the top of AMS in units of  $[m^2 \text{ sr s GeV}]^{-1}$ . Characteristic energy  $\tilde{E}$  (i.e. spectrally weighted mean energy in the bin) is given with its systematic error from the energy scale uncertainty. The number of positron events before unfolding,  $N_{e^+}$ , is given together with its statistical error from the fit.  $\sigma_{\text{stat}}$  is the statistical error.  $\sigma_{\text{syst}}^{\text{tmpl}}$  is the systematic error from the definition of templates.  $\sigma_{\text{syst}}^{\text{c.c.}}$  is the systematic error from the charge confusion.  $\sigma_{\text{syst}}^{\text{eff}}$  is the systematic error from the efficiency corrections.  $\sigma_{\text{syst}}^{\text{unf}}$  is the systematic error from the unfolding.  $\sigma_{\text{syst}}$  is the total systematic error, which is equal to the sum of  $\sigma_{\text{syst}}^{\text{tmpl}}$ ,  $\sigma_{\text{syst}}^{\text{c.c.}}$ ,  $\sigma_{\text{syst}}^{\text{eff}}$ , and  $\sigma_{\text{syst}}^{\text{unf}}$  in quadrature.  $\sigma_{\text{syst}}^{\text{eff}}$  includes the correlated systematic error on the flux normalization of 1%. Note that this 1% error is subtracted in quadrature from the total systematic error for all the fits in this Letter.

$E$ [GeV]	$\tilde{E}$ [GeV]	$N_{e^+}$	$\Phi_{e^+}$	$\sigma_{\text{stat}}$	$\sigma_{\text{syst}}^{\text{tmpl}}$	$\sigma_{\text{syst}}^{\text{c.c.}}$	$\sigma_{\text{syst}}^{\text{acc}}$	$\sigma_{\text{syst}}^{\text{unf}}$	$\sigma_{\text{syst}}$
0.50 - 0.65	$0.57 \pm 0.02$	$1149 \pm 47$	(2.669 0.109 0.075 0.000 0.107 0.053 0.141)	$\times 10^0$					
0.65 - 0.82	$0.73 \pm 0.02$	$12911 \pm 144$	(2.576 0.029 0.046 0.000 0.083 0.044 0.105)	$\times 10^0$					
0.82 - 1.01	$0.91 \pm 0.03$	$26583 \pm 192$	(2.272 0.016 0.022 0.000 0.060 0.031 0.071)	$\times 10^0$					
1.01 - 1.22	$1.11 \pm 0.03$	$40179 \pm 225$	(1.929 0.011 0.013 0.000 0.043 0.019 0.049)	$\times 10^0$					
1.22 - 1.46	$1.33 \pm 0.03$	$54417 \pm 254$	(1.528 0.007 0.009 0.000 0.027 0.014 0.032)	$\times 10^0$					
1.46 - 1.72	$1.58 \pm 0.04$	$74795 \pm 293$	(1.196 0.005 0.006 0.000 0.018 0.009 0.021)	$\times 10^0$					
1.72 - 2.00	$1.85 \pm 0.04$	$94015 \pm 326$	(9.239 0.032 0.038 0.002 0.120 0.059 0.139)	$\times 10^{-1}$					
2.00 - 2.31	$2.15 \pm 0.05$	$109166 \pm 349$	(7.003 0.022 0.028 0.002 0.084 0.035 0.095)	$\times 10^{-1}$					
2.31 - 2.65	$2.47 \pm 0.05$	$117702 \pm 363$	(5.341 0.016 0.022 0.001 0.059 0.025 0.068)	$\times 10^{-1}$					
2.65 - 3.00	$2.82 \pm 0.06$	$113376 \pm 357$	(3.983 0.013 0.016 0.001 0.043 0.017 0.049)	$\times 10^{-1}$					
3.00 - 3.36	$3.17 \pm 0.06$	$106314 \pm 345$	(3.024 0.010 0.012 0.001 0.032 0.012 0.036)	$\times 10^{-1}$					
3.36 - 3.73	$3.54 \pm 0.07$	$98881 \pm 334$	(2.338 0.008 0.010 0.001 0.024 0.009 0.028)	$\times 10^{-1}$					
3.73 - 4.12	$3.92 \pm 0.08$	$92976 \pm 323$	(1.809 0.006 0.007 0.001 0.019 0.007 0.021)	$\times 10^{-1}$					
4.12 - 4.54	$4.32 \pm 0.08$	$87849 \pm 315$	(1.389 0.005 0.006 0.000 0.015 0.005 0.016)	$\times 10^{-1}$					
4.54 - 5.00	$4.76 \pm 0.09$	$84539 \pm 308$	(1.069 0.004 0.004 0.000 0.011 0.004 0.013)	$\times 10^{-1}$					
5.00 - 5.49	$5.24 \pm 0.10$	$79695 \pm 300$	(8.208 0.031 0.034 0.003 0.088 0.028 0.099)	$\times 10^{-2}$					
5.49 - 6.00	$5.74 \pm 0.11$	$72564 \pm 287$	(6.278 0.025 0.026 0.002 0.068 0.021 0.076)	$\times 10^{-2}$					
6.00 - 6.54	$6.26 \pm 0.12$	$67597 \pm 276$	(4.923 0.020 0.021 0.002 0.054 0.015 0.060)	$\times 10^{-2}$					
6.54 - 7.10	$6.81 \pm 0.13$	$60745 \pm 261$	(3.890 0.017 0.017 0.001 0.043 0.012 0.048)	$\times 10^{-2}$					
7.10 - 7.69	$7.39 \pm 0.14$	$53538 \pm 246$	(3.018 0.014 0.013 0.001 0.034 0.009 0.037)	$\times 10^{-2}$					
7.69 - 8.30	$7.99 \pm 0.15$	$47132 \pm 230$	(2.406 0.012 0.010 0.001 0.027 0.006 0.030)	$\times 10^{-2}$					
8.30 - 8.95	$8.62 \pm 0.16$	$42041 \pm 218$	(1.900 0.010 0.008 0.001 0.022 0.005 0.024)	$\times 10^{-2}$					
8.95 - 9.62	$9.28 \pm 0.18$	$36843 \pm 203$	(1.530 0.008 0.007 0.001 0.018 0.004 0.019)	$\times 10^{-2}$					
9.62 - 10.32	$9.96 \pm 0.19$	$32889 \pm 193$	(1.242 0.007 0.005 0.000 0.015 0.003 0.016)	$\times 10^{-2}$					
10.32 - 11.04	$10.67 \pm 0.20$	$28518 \pm 179$	(1.007 0.006 0.004 0.000 0.012 0.002 0.013)	$\times 10^{-2}$					
11.04 - 11.80	$11.41 \pm 0.22$	$25852 \pm 170$	(8.302 0.055 0.037 0.003 0.100 0.017 0.108)	$\times 10^{-3}$					
11.80 - 12.59	$12.19 \pm 0.23$	$23378 \pm 162$	(6.918 0.048 0.031 0.002 0.084 0.014 0.090)	$\times 10^{-3}$					
12.59 - 13.41	$12.99 \pm 0.25$	$20709 \pm 152$	(5.668 0.042 0.025 0.002 0.069 0.011 0.075)	$\times 10^{-3}$					
13.41 - 14.25	$13.82 \pm 0.26$	$18103 \pm 142$	(4.643 0.037 0.021 0.002 0.057 0.009 0.061)	$\times 10^{-3}$					
14.25 - 15.14	$14.69 \pm 0.28$	$16624 \pm 137$	(3.864 0.032 0.017 0.001 0.048 0.008 0.051)	$\times 10^{-3}$					
15.14 - 16.05	$15.59 \pm 0.29$	$15015 \pm 130$	(3.262 0.028 0.015 0.001 0.041 0.007 0.044)	$\times 10^{-3}$					
16.05 - 17.00	$16.52 \pm 0.31$	$13638 \pm 124$	(2.718 0.025 0.012 0.001 0.034 0.005 0.037)	$\times 10^{-3}$					
17.00 - 17.98	$17.48 \pm 0.33$	$12414 \pm 118$	(2.293 0.022 0.011 0.001 0.029 0.005 0.031)	$\times 10^{-3}$					

Continued on next page

TABLE SI – (*Continued*).

E [GeV]	$\tilde{E}$ [GeV]	$N_{e+}$	$\Phi_{e+}$	$\sigma_{\text{stat}}$	$\sigma_{\text{syst}}^{\text{tmpl}}$	$\sigma_{\text{syst}}^{\text{c.c.}}$	$\sigma_{\text{syst}}^{\text{acc}}$	$\sigma_{\text{syst}}^{\text{unf}}$	$\sigma_{\text{syst}}$
17.98 - 18.99	$18.48 \pm 0.35$	$11371 \pm 113$	(1.933 0.019 0.009 0.001 0.025 0.004 0.026)	$\times 10^{-3}$					
18.99 - 20.04	$19.51 \pm 0.37$	$10708 \pm 110$	(1.666 0.017 0.008 0.001 0.021 0.003 0.023)	$\times 10^{-3}$					
20.04 - 21.13	$20.58 \pm 0.39$	$9985 \pm 106$	(1.454 0.015 0.007 0.000 0.019 0.003 0.020)	$\times 10^{-3}$					
21.13 - 22.25	$21.68 \pm 0.41$	$8861 \pm 100$	(1.214 0.014 0.006 0.000 0.016 0.002 0.017)	$\times 10^{-3}$					
22.25 - 23.42	$22.83 \pm 0.43$	$7974 \pm 95$	(1.018 0.012 0.005 0.000 0.013 0.002 0.014)	$\times 10^{-3}$					
23.42 - 24.62	$24.01 \pm 0.45$	$7434 \pm 91$	(9.031 0.111 0.043 0.003 0.118 0.018 0.127)	$\times 10^{-4}$					
24.62 - 25.90	$25.25 \pm 0.48$	$6859 \pm 88$	(7.647 0.098 0.037 0.002 0.100 0.015 0.108)	$\times 10^{-4}$					
25.90 - 27.25	$26.56 \pm 0.50$	$6516 \pm 86$	(6.757 0.089 0.033 0.002 0.089 0.014 0.096)	$\times 10^{-4}$					
27.25 - 28.68	$27.95 \pm 0.53$	$5881 \pm 82$	(5.747 0.080 0.028 0.002 0.076 0.011 0.082)	$\times 10^{-4}$					
28.68 - 30.21	$29.43 \pm 0.56$	$5541 \pm 79$	(5.063 0.072 0.025 0.001 0.067 0.010 0.072)	$\times 10^{-4}$					
30.21 - 31.82	$31.00 \pm 0.59$	$4902 \pm 75$	(4.273 0.065 0.022 0.001 0.057 0.009 0.061)	$\times 10^{-4}$					
31.82 - 33.53	$32.66 \pm 0.62$	$4487 \pm 72$	(3.681 0.059 0.019 0.001 0.049 0.007 0.053)	$\times 10^{-4}$					
33.53 - 35.36	$34.43 \pm 0.65$	$4059 \pm 68$	(3.126 0.052 0.016 0.001 0.042 0.006 0.045)	$\times 10^{-4}$					
35.36 - 37.31	$36.32 \pm 0.69$	$3810 \pm 66$	(2.754 0.048 0.015 0.001 0.037 0.006 0.040)	$\times 10^{-4}$					
37.31 - 39.39	$38.33 \pm 0.72$	$3423 \pm 63$	(2.328 0.043 0.013 0.001 0.031 0.005 0.034)	$\times 10^{-4}$					
39.39 - 41.61	$40.48 \pm 0.77$	$3142 \pm 60$	(2.004 0.038 0.011 0.001 0.027 0.004 0.030)	$\times 10^{-4}$					
41.61 - 44.00	$42.78 \pm 0.81$	$2897 \pm 58$	(1.723 0.034 0.010 0.000 0.023 0.003 0.026)	$\times 10^{-4}$					
44.00 - 46.57	$45.26 \pm 0.86$	$2607 \pm 55$	(1.446 0.030 0.009 0.000 0.020 0.003 0.022)	$\times 10^{-4}$					
46.57 - 49.33	$47.92 \pm 0.91$	$2558 \pm 54$	(1.323 0.028 0.009 0.000 0.018 0.003 0.020)	$\times 10^{-4}$					
49.33 - 52.33	$50.80 \pm 0.96$	$2155 \pm 50$	(1.029 0.024 0.007 0.000 0.014 0.002 0.016)	$\times 10^{-4}$					
52.33 - 55.58	$53.92 \pm 1.02$	$2005 \pm 48$	(8.860 0.214 0.063 0.002 0.121 0.018 0.137)	$\times 10^{-5}$					
55.58 - 59.13	$57.32 \pm 1.08$	$1864 \pm 47$	(7.558 0.189 0.056 0.002 0.103 0.015 0.118)	$\times 10^{-5}$					
59.13 - 63.02	$61.03 \pm 1.16$	$1645 \pm 44$	(6.115 0.164 0.047 0.001 0.084 0.012 0.097)	$\times 10^{-5}$					
63.02 - 67.30	$65.11 \pm 1.23$	$1626 \pm 44$	(5.502 0.149 0.044 0.001 0.075 0.011 0.088)	$\times 10^{-5}$					
67.30 - 72.05	$69.62 \pm 1.32$	$1427 \pm 41$	(4.367 0.126 0.036 0.001 0.060 0.009 0.071)	$\times 10^{-5}$					
72.05 - 77.37	$74.65 \pm 1.41$	$1399 \pm 41$	(3.826 0.111 0.033 0.001 0.052 0.008 0.062)	$\times 10^{-5}$					
77.37 - 83.36	$80.29 \pm 1.52$	$1234 \pm 38$	(3.013 0.094 0.027 0.001 0.041 0.006 0.050)	$\times 10^{-5}$					
83.36 - 90.19	$86.69 \pm 1.64$	$1168 \pm 38$	(2.511 0.081 0.024 0.002 0.034 0.005 0.042)	$\times 10^{-5}$					
90.19 - 98.08	$94.02 \pm 1.78$	$1090 \pm 36$	(2.037 0.068 0.020 0.001 0.028 0.004 0.035)	$\times 10^{-5}$					
98.1 - 107.3	$102.6 \pm 1.9$	$913 \pm 37$	(1.461 0.059 0.015 0.002 0.020 0.003 0.025)	$\times 10^{-5}$					
107.3 - 118.4	$112.7 \pm 2.1$	$871 \pm 36$	(1.173 0.048 0.012 0.001 0.016 0.002 0.020)	$\times 10^{-5}$					
118.4 - 132.1	$125.0 \pm 2.4$	$789 \pm 34$	(8.677 0.376 0.090 0.014 0.120 0.017 0.151)	$\times 10^{-6}$					
132.1 - 148.8	$140.1 \pm 2.7$	$741 \pm 32$	(6.998 0.303 0.075 0.012 0.099 0.014 0.125)	$\times 10^{-6}$					
148.8 - 169.9	$158.9 \pm 3.0$	$613 \pm 30$	(4.595 0.221 0.051 0.012 0.065 0.009 0.084)	$\times 10^{-6}$					
169.9 - 197.7	$183.1 \pm 3.5$	$556 \pm 28$	(3.201 0.163 0.037 0.011 0.046 0.006 0.060)	$\times 10^{-6}$					
197.7 - 237.2	$216.2 \pm 4.2$	$405 \pm 24$	(1.871 0.111 0.022 0.012 0.029 0.004 0.039)	$\times 10^{-6}$					
237.2 - 290.0	$261.8 \pm 5.1$	$330 \pm 22$	(1.158 0.077 0.014 0.012 0.019 0.002 0.026)	$\times 10^{-6}$					
290.0 - 370.0	$326.8 \pm 6.4$	$214 \pm 18$	(5.773 0.496 0.071 0.089 0.097 0.012 0.150)	$\times 10^{-7}$					
370.0 - 500.0	$428.5 \pm 8.6$	$146 \pm 17$	(2.491 0.286 0.031 0.072 0.045 0.005 0.091)	$\times 10^{-7}$					
500.0 - 700.0	$588.8 \pm 12.2$	$71 \pm 14$	(8.312 1.675 0.548 0.512 0.175 0.017 0.770)	$\times 10^{-8}$					
700.0 - 1000.0	$832.3 \pm 18.3$	$23 \pm 13$	(1.927 1.087 0.258 0.358 0.049 0.004 0.444)	$\times 10^{-8}$					

TABLE SII. The fit parameters corresponding to the fit of Eq. (4) to the positron flux in the energy range [0.5 – 1000] GeV. Note that parameters  $\varphi_{e^+}$ ,  $C_d$  and  $\gamma_d$  are the average values over the time period covered in the Letter. For the time variation of these parameters see Fig. S6.

Parameter	Value	$\sigma$	Units
$1/E_s$	1.23	$\pm 0.34$	$\text{TeV}^{-1}$
$C_s$	(6.80 $\pm 0.15$ )	$\times 10^{-5} [\text{m}^2 \text{sr s GeV}]^{-1}$	
$\gamma_s$	-2.58	$\pm 0.05$	
$C_d$	(6.51 $\pm 0.14$ )	$\times 10^{-2} [\text{m}^2 \text{sr s GeV}]^{-1}$	
$\gamma_d$	-4.07	$\pm 0.06$	
$\varphi_{e^+}$	1.10	$\pm 0.03$	GeV

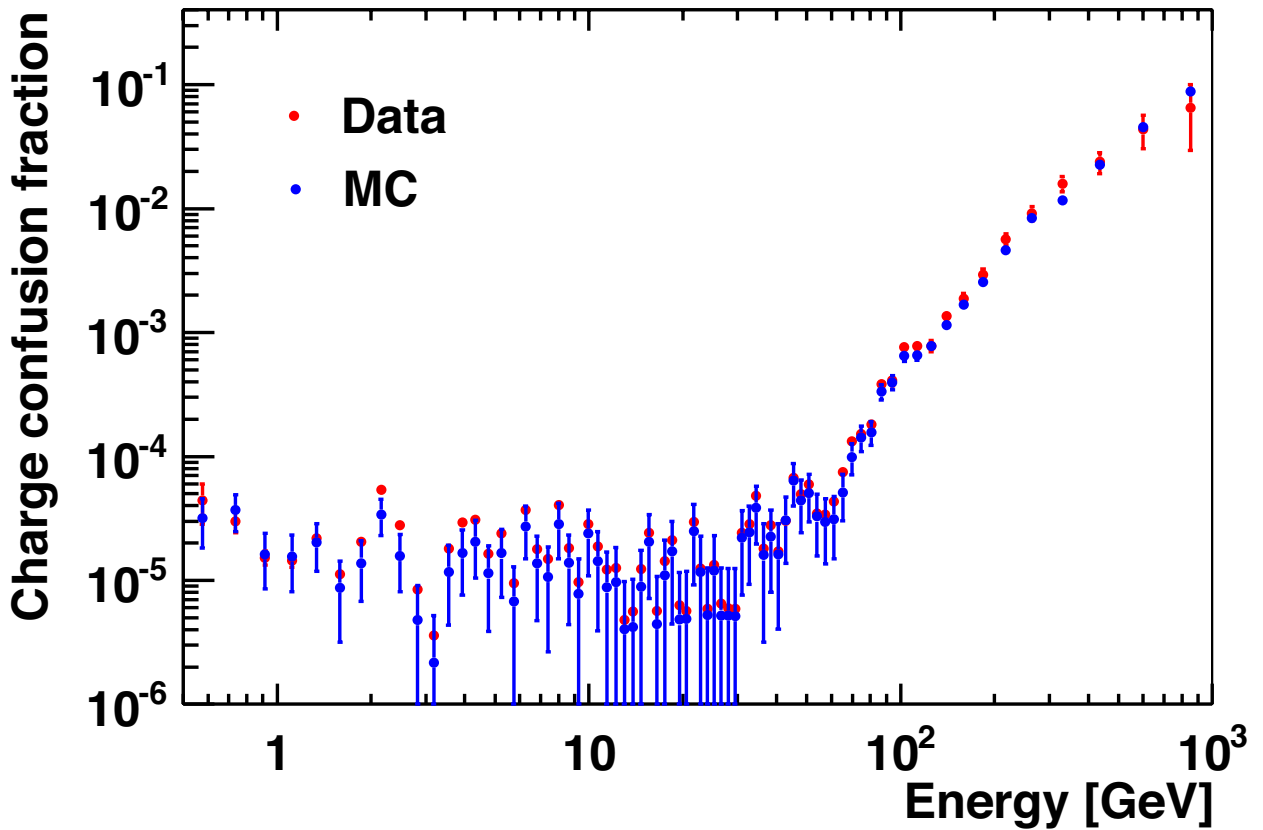


FIG. S1. The measured electron charge confusion fraction for  $\Lambda_{\text{CC}}^e > 0$  as a function of electron energy. The charge confusion fraction is less than 8% in the energy range of the Letter.

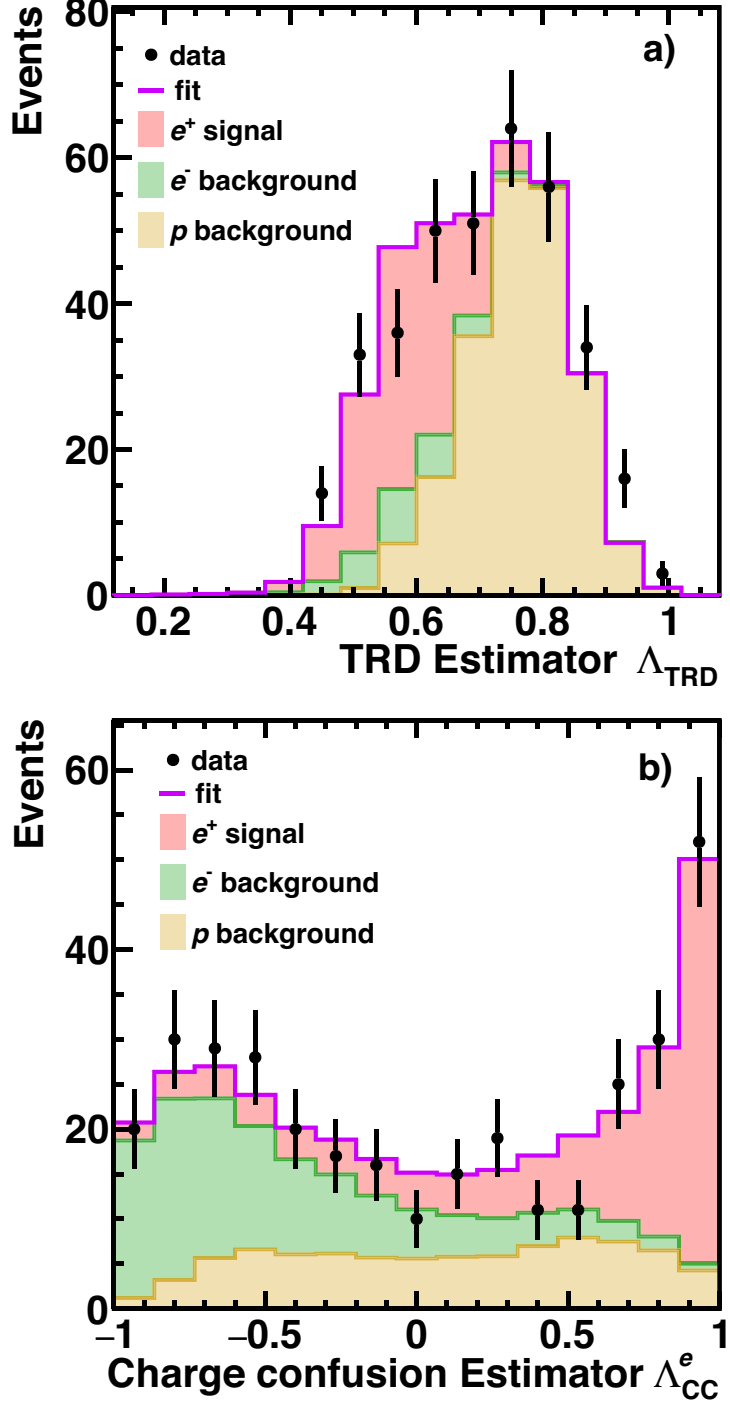


FIG. S2. An illustration of the fit to the data in the energy range [370 – 500] GeV. The  $\chi^2/\text{d.o.f.}$  of the fit is 209/207. The projections of the 2D data distribution (black data points) to the (a)  $\Lambda_{\text{TRD}}$  and (b)  $\Lambda_{\text{CC}}^e$  axes are shown together with the signal and background contributions: the positron signal template (red), the proton background template (tan), and the charge confusion electron background template (green). In this illustration the projection onto the  $\Lambda_{\text{TRD}}$  axis uses a cut  $\Lambda_{\text{CC}}^e > 0.0$  and the projection onto the  $\Lambda_{\text{CC}}^e$  axis uses a cut  $\Lambda_{\text{TRD}} < 0.7$ . These cuts are applied for demonstration purposes only, such that  $\sim 90\%$  of the signal events quoted in Table SMI are shown in these plots.

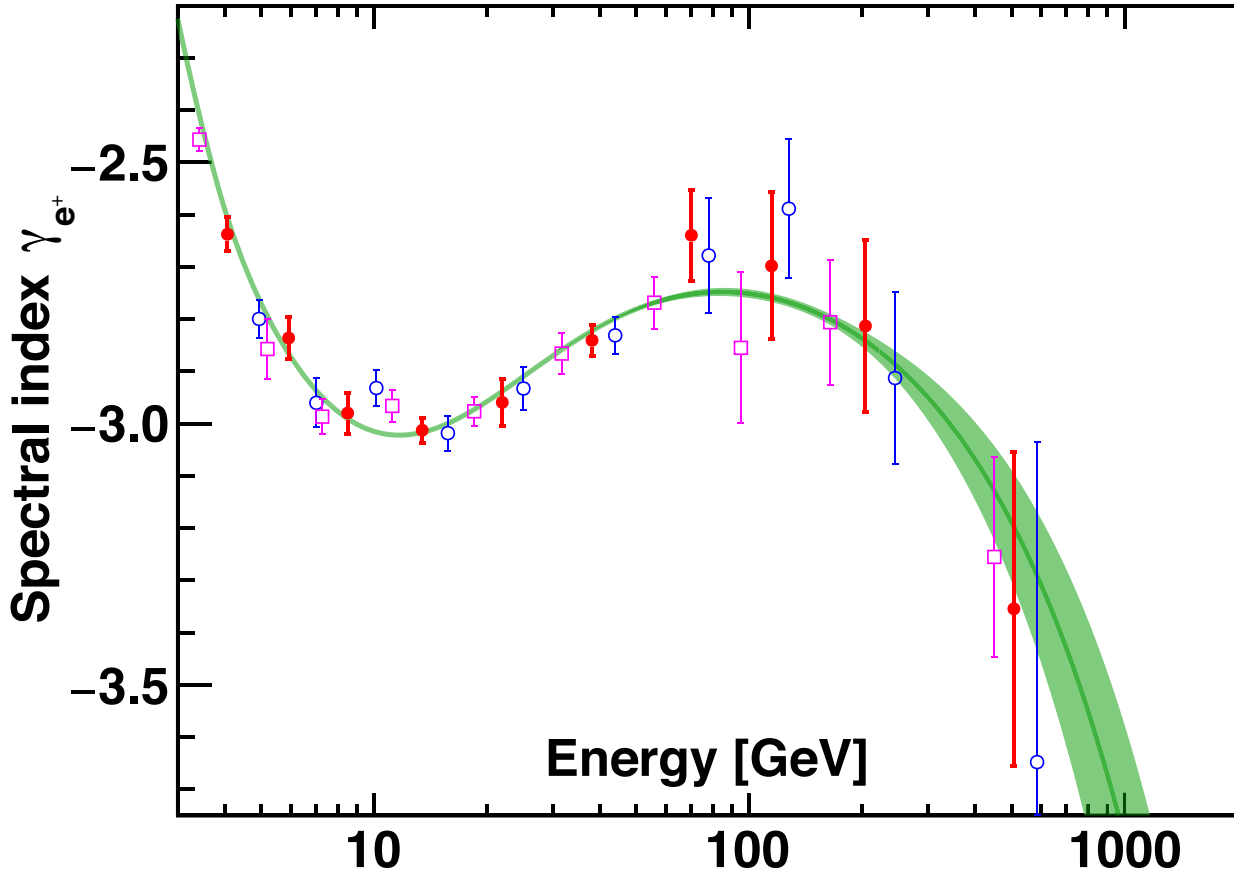


FIG. S3. The positron spectral index in non-overlapping energy intervals. The filled red circles correspond to the energy ranges in the text, the open blue circles correspond to the energy ranges shifted by one or two energy bins to the right, and open magenta squares correspond to the energy ranges shifted by one or two bins to the left. The green band represents the 68% CL interval of the minimal model fit of Eq. (4) to the positron flux (see text).

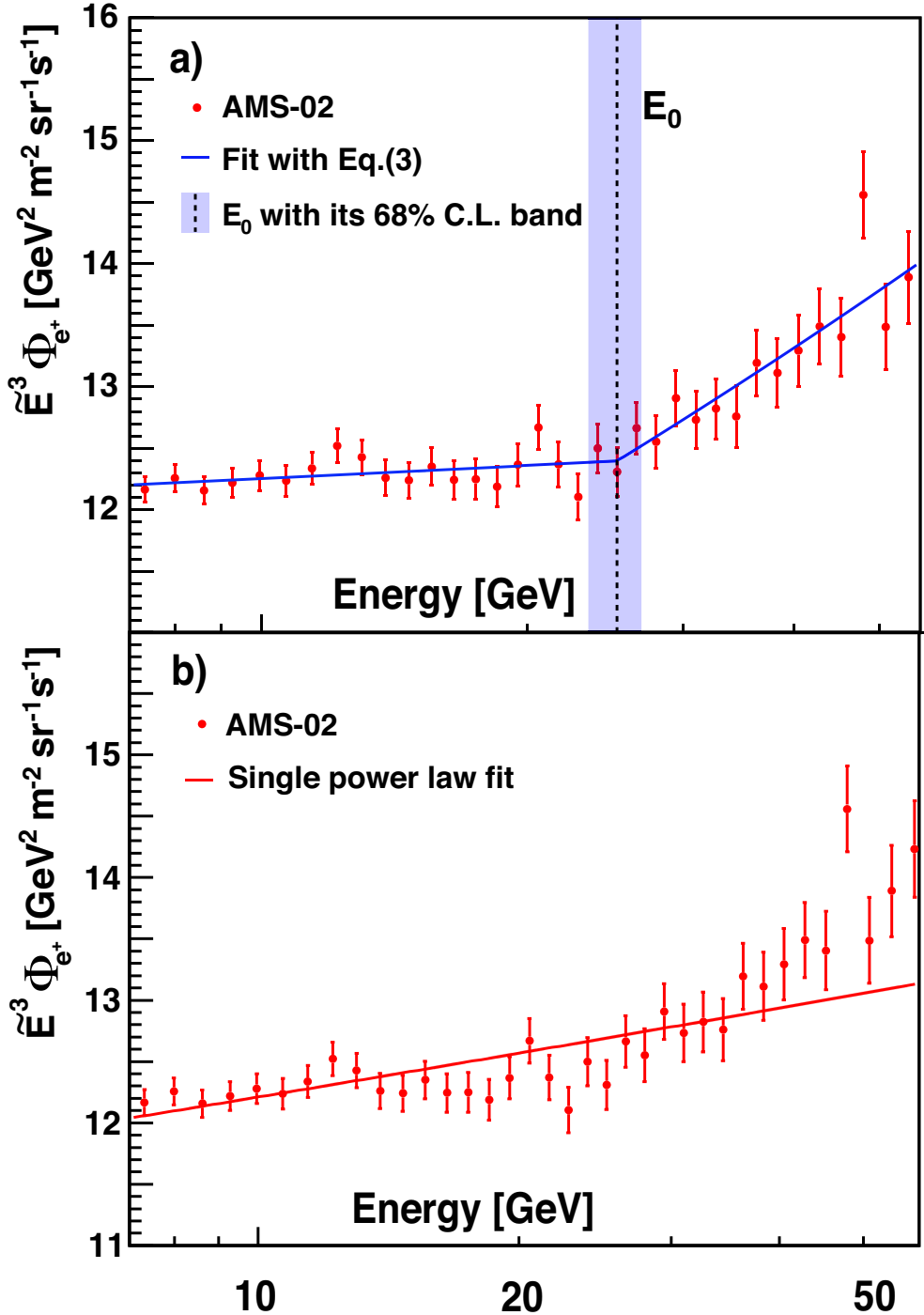


FIG. S4. To study the significance of the spectral index increase (hardening) at  $E_0 = 25.2 \pm 1.8$  GeV we test two hypotheses for the positron spectrum (red data points) in the energy range [7.10 – 55.58] GeV: (a) a double power law function, Eq. (3), with the fit yielding  $\chi^2/\text{d.o.f.} = 22.8/31$  (blue line); and (b) a single power law function,  $\Phi_{e^+}(E) = C(E/55.58\text{ GeV})^\gamma$ , with the fit yielding  $\chi^2/\text{d.o.f.} = 67.2/33$  (red line). This excludes the single power law hypothesis at the  $6.35\sigma$  level.

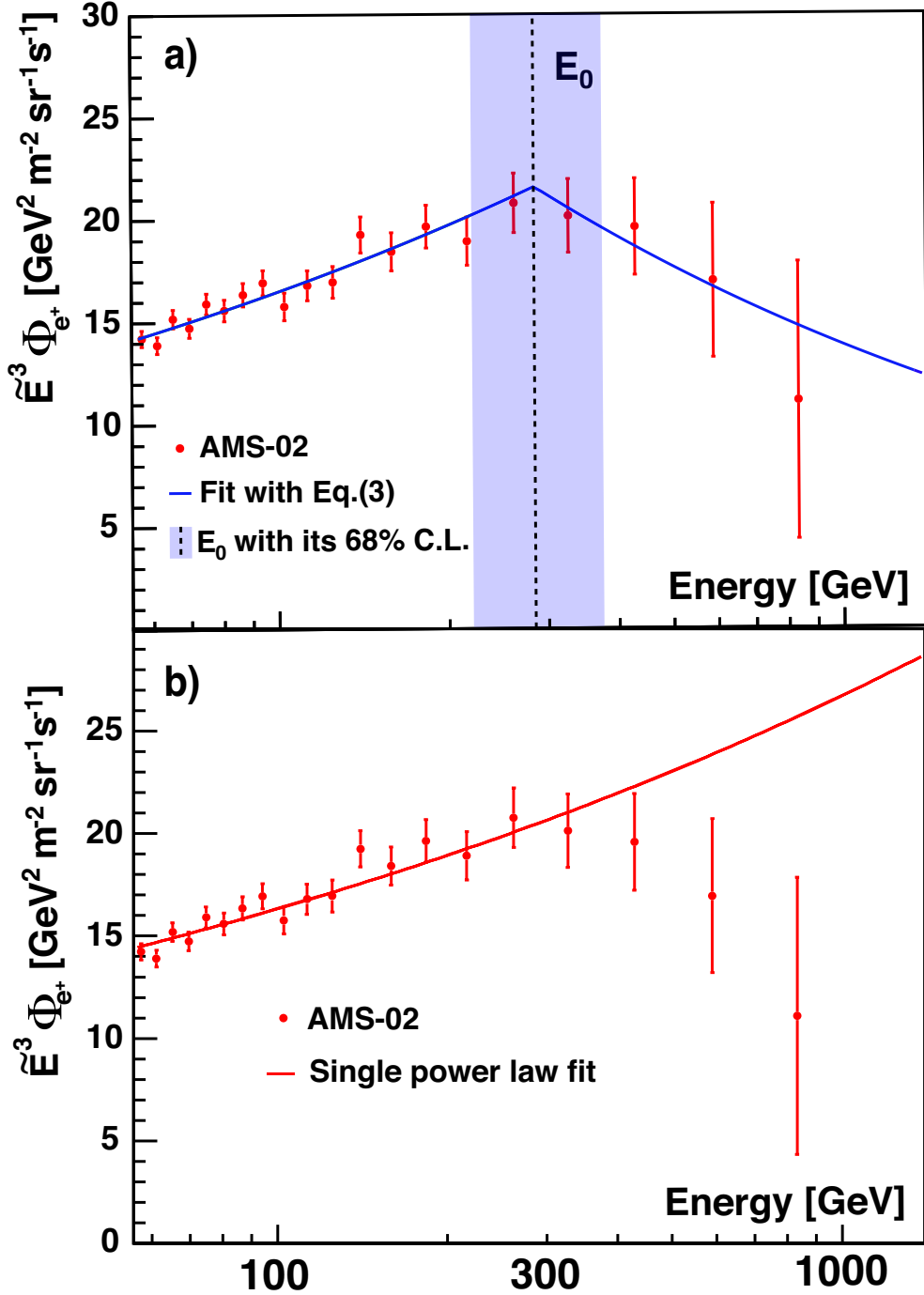


FIG. S5. To study the significance of the spectral index decrease (softening) at  $284^{+91}_{-64}$  GeV we test two hypotheses for the positron spectrum (red data points) in the energy range [55.58 – 1000] GeV: (a) a double power law function, Eq. (3), with the fit yielding  $\chi^2/\text{d.o.f.} = 12.9/16$  (blue line); and (b) a single power law function,  $\Phi_{e^+}(E) = C(E/55.58 \text{ GeV})^\gamma$ , with the fit yielding  $\chi^2/\text{d.o.f.} = 24.9/18$  (red line). This excludes the single power law hypothesis at the  $3.04\sigma$  level.

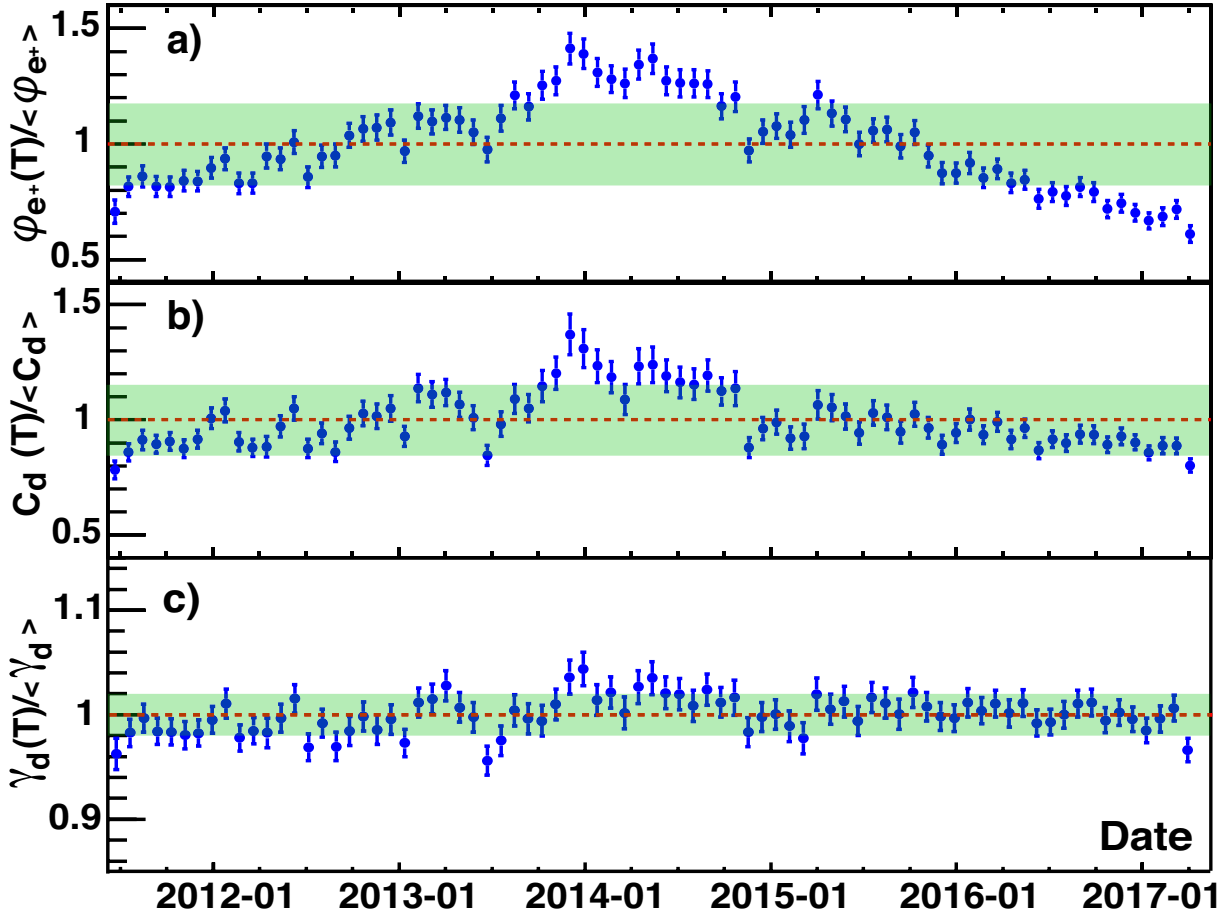


FIG. S6. To study the time dependence of the fit parameters, we performed fits of Eq. (4) to independent data samples corresponding to a single Bartels rotation [3]. The variation of the  $\chi^2$  of these fits is negligible if the source term parameters,  $C_s$ ,  $\gamma_s$ , and  $1/E_s$ , are left to vary freely in the fit or fixed to the values in Table SII. This is consistent with the observation that the positron spectrum is time independent for energies above 20 GeV [3]. For the other parameters,  $\varphi_{e^+}$ ,  $C_d$  and  $\gamma_d$ , there is significant increase of the  $\chi^2$  if these parameters are fixed to the Table SII values. Therefore, we fix source term parameters  $C_s$ ,  $\gamma_s$ , and  $1/E_s$  to their values in Table SII and determine the remaining parameters for each Bartels rotation: (a) solar modulation parameter  $\varphi_{e^+}$ ; (b) diffuse term normalization  $C_d$ ; and (c) diffuse term spectral index  $\gamma_d$ . All parameters are divided by their respective average values to show their relative variation due to time dependent solar effects. The horizontal bands represent the r.m.s. variation of the corresponding parameter over the measurement period. As seen there is a significant variation of the parameters  $\varphi_{e^+}$  and  $C_d$ , whereas  $\gamma_d$  does not have a sizeable time dependence.